

Supporting Information

FRET based fluorescence ratiometric and colorimetric sensor to discriminate Fe³⁺ from Fe²⁺

Sangita Das^a, Krishnendu Aich^a, Shyamaprosad Goswami,^{*a} Ching Kheng Quah^b and Hoong-Kun Fun^{b,c}

^a Department of Chemistry, Indian Institute of Engineering Science and Technology, Shibpur, Howrah-711 103, India. Fax: +91 33 2668 2916; Tel: +91 33 2668 2961-3; E-mail: spgoswamical@yahoo.com

^bX-ray Crystallography Unit, School of Physics, Universiti Sains Malaysia, 11800 USM, Penang, Malaysia.

^cDepartment of Pharmaceutical Chemistry, College of Pharmacy, King Saud University, Riyadh 11451, Saudi Arabia

CONTENTS

1. Determination of detection limit.....	
2. Determination of association constant.....	
3. X-ray crystallographic data.....	
4. ¹ H NMR spectrum of Compound 1.....	
5. ¹³ C NMR spectrum of Compound 1	
6. Mass spectrum (HRMS) of Compound 1	
7. ¹ H NMR spectrum of RQBTE.....	
8. ¹³ C NMR spectrum of RQBTE.....	
9. Mass spectrum (HRMS) of RQBTE	
10. Mass spectrum (HRMS) of RQBTE-Fe ³⁺	

1. Determination of detection limit

The detection limit was calculated based on the fluorescence titration. To determine the S/N ratio, the absorbance of RQBTE without Fe^{3+} was measured by 10 times and the standard deviation of blank measurements was determined. The detection limit (DL) of **RQBTE** for Fe^{3+} was determined from the following equation: $\text{DL} = K \times \text{Sb}_1 / S$

Where $K = 2$ or 3 (we take 3 in this case); Sb_1 is the standard deviation of the blank solution; S is the slope of the calibration curve. From the graph we get slope = 96705.429 , and Sb_1 value is 0.00174 . Thus using the formula we get the Detection Limit = 5.39×10^{-8} M i.e. RQBTE can detect Fe^{3+} in this minimum concentration by fluorescence techniques.

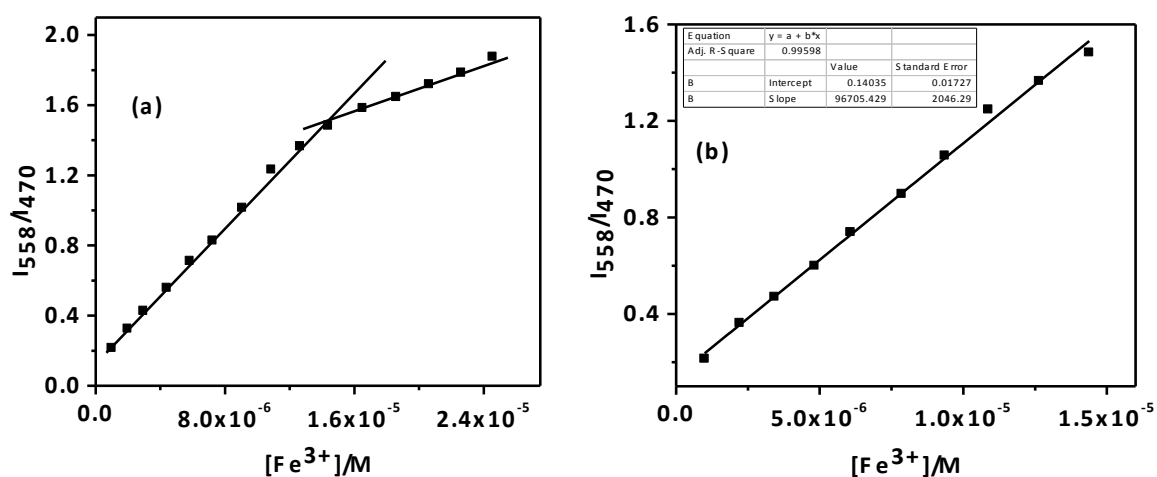


Figure S1: Fluorescence (a) Response and (b) only linear curve of RQBTE at fluorescence intensity ratio (I_{558}/I_{470}) nm depending on Fe^{3+} concentration.

Linear responsive curve of RQBTE in presence of Fe^{3+}

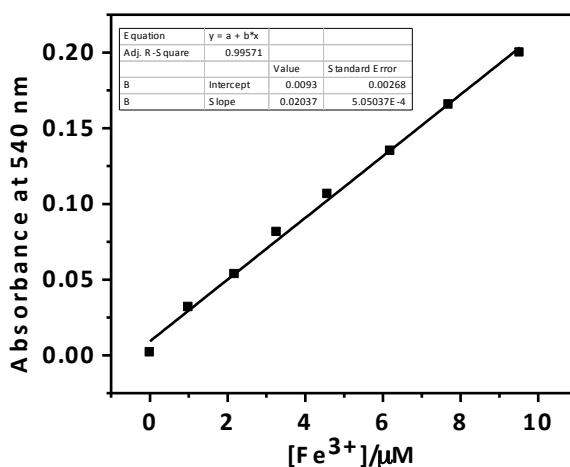


Figure S2: UV-vis Response curve of RQBTE at 540 nm depending on Fe^{3+} concentration.

2. Determination of Association Constant (K_a)

By fluorescence method:

Association constant was calculated according to the Benesi-Hildebrand equation. K_a was calculated following the equation stated below.

$$1/(I-I_0) = 1/\{K(I_{\max}-I_0) [M^{X^+}]^n\} + 1/[I_{\max}-I_0]$$

Here I_0 is the fluorescence of receptor in the absence of guest, I is the fluorescence recorded in the presence of added guest, I_{\max} is fluorescence in presence of added $[M^{X^+}]_{\max}$ and K_a is the association constant, where $[M^{X^+}]$ is $[Fe^{3+}]$. The association constant (K_a) could be determined from the slope of the straight line of the plot of $1/(I-I_0)$ against $1/[Fe^{3+}]$ and is found to be $6.12 \times 10^5 M^{-1}$.

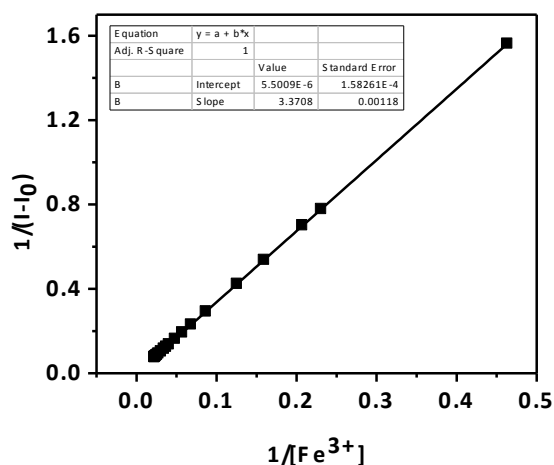


Figure S3: Benesi-Hildebrand plot from absorption titration data of receptor (RQBTE, 10 μ M) with Fe^{3+} .

3. X-ray crystallographic data

X-ray diffraction data of a single crystal of **RQBTE** (with dimensions of $0.38 \times 0.25 \times 0.09$ mm) was collected on Bruker APEX II Duo CCD area-detector diffractometer operating at 50kV and 30mA using Mo $K\alpha$ radiation ($\lambda = 0.71073$ Å). Diffraction data were collected with the Oxford Cryosystem Cobra low temperature attachment at 100.0 (1) K [1]. Data collection and reduction were performed using the APEX2 and SAINT software [2]. The SADABS software was used for absorption correction [2]. **RQBTE** was solved by direct method and refinement was carried out by the full-matrix least-squares technique on F^2 using SHELXTL package [3]. All non-hydrogen atoms were refined anisotropically whereas hydrogen atoms were refined isotropically. N-bound H atoms were located in the difference Fourier map and refined freely [N—H = 0.82 (2) - 0.88 (2) Å]. The remaining H atoms were placed in calculated positions with C—H = 0.95 - 0.99 Å after checking their positions in the

Fourier difference map. The U_{iso} values were constrained to be 1.2 or 1.5 U_{eq} of the carrier atom. A rotating-group model was applied for the methyl groups. The crystallographic data and hydrogen bonds geometry are presented in Table S1 and S2, respectively. Crystallographic data for **RQBTE** has been deposited with the Cambridge Crystallographic Data Center No. CCDC 1416906. Copy of the data can be obtained free of charge on application to the CCDC, 12 Union Road, Cambridge CB2 IEZ, UK. Fax: +44-(0)1223-336033 or E-Mail: deposit@ccdc.cam.ac.uk.

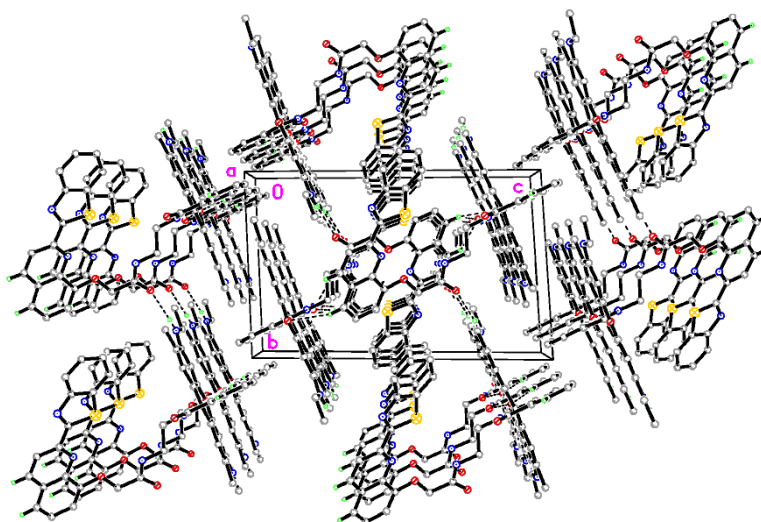


Figure S4: The crystal packing of **RQBTE** viewed along the a -axis and H atoms not involved in intermolecular interactions (dashed lines) have been omitted for clarity.

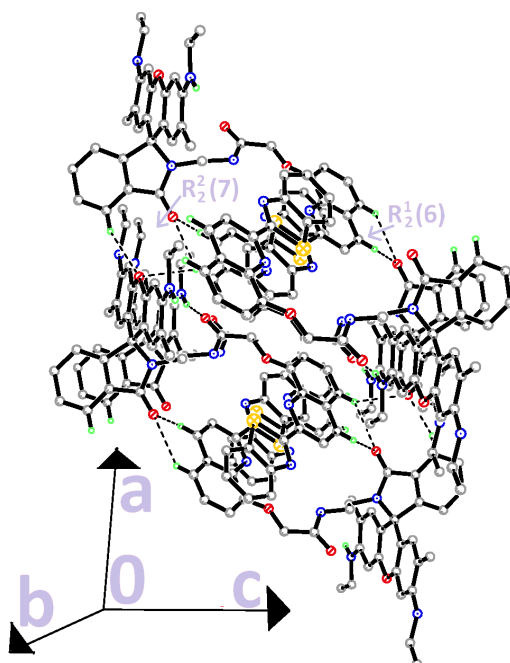


Figure S5: Part of the crystal packing of **RQBTE** viewed along [010], showing the $R_2^2(7)$ and $R_2^1(6)$ ring motifs.

Table S1 Experimental details

Crystal data (CCDC 1416906)	
Chemical formula	C ₄₆ H ₄₂ N ₆ O ₄ S
<i>M</i> _r	774.91
Crystal system, space group	Triclinic, <i>P</i> $\bar{1}$
Temperature (K)	100
<i>a</i> , <i>b</i> , <i>c</i> (Å)	9.0642 (11), 11.8519 (14), 18.732 (2)
α , β , γ (°)	86.072 (2), 83.458 (2), 81.905 (2)
<i>V</i> (Å ³)	1976.4 (4)
<i>Z</i>	2
Radiation type	Mo <i>K</i> α
μ (mm ⁻¹)	0.14
Crystal size (mm)	0.38 × 0.25 × 0.09
Data collection	
Diffractometer	Bruker <i>SMART APEX II</i> DUO CCD area-detector diffractometer
Absorption correction	Multi-scan (<i>SADABS</i> ; Bruker, 2009)
<i>T</i> _{min} , <i>T</i> _{max}	0.950, 0.988
No. of measured, independent and observed [<i>I</i> > 2σ(<i>I</i>)] reflections	34021, 7909, 5676
<i>R</i> _{int}	0.060

$(\sin \theta/\lambda)_{\max}$ (\AA^{-1})	0.622
Refinement	
$R[F^2 > 2\sigma(F^2)], wR(F^2), S$	0.048, 0.119, 1.02
No. of reflections	7909
No. of parameters	530
H-atom treatment	H atoms treated by a mixture of independent and constrained refinement
$\Delta\rho_{\max}, \Delta\rho_{\min}$ ($e \text{\AA}^{-3}$)	0.31, -0.33

Table S2 Hydrogen-bond geometry ($\text{\AA}, ^\circ$)

$D-H\cdots A$	$D-H$	$H\cdots A$	$D\cdots A$	$D-H\cdots A$
$N5-H1N5\cdots O3^i$	0.86 (2)	2.16 (2)	2.988 (2)	161 (2)
$C18-H18A\cdots O1^{ii}$	0.95	2.53	3.418 (2)	157
$C28-H28A\cdots O1^{iii}$	0.95	2.60	3.384 (3)	141
$C28-H28A\cdots O2^{iv}$	0.95	2.59	3.358 (3)	138
$C30-H30A\cdots O2^{iv}$	0.95	2.37	3.190 (3)	144
$C16-H16A\cdots Cg1^v$	0.95	2.55	3.486 (2)	168
$C46-H46C\cdots Cg2^{vi}$	0.98	2.84	3.483 (2)	124

Symmetry codes: (i) $x, y+1, z$; (ii) $x-1, y, z$; (iii) $-x+1, -y+1, -z+1$; (iv) $-x, -y+1, -z+1$; (v) $-x+1, -y+2, -z$; (vi) $-x+1, -y+1, -z$.

* Cg 1 and Cg2 are the centroids for C1—C6 and C14—C19 benzene rings, respectively.

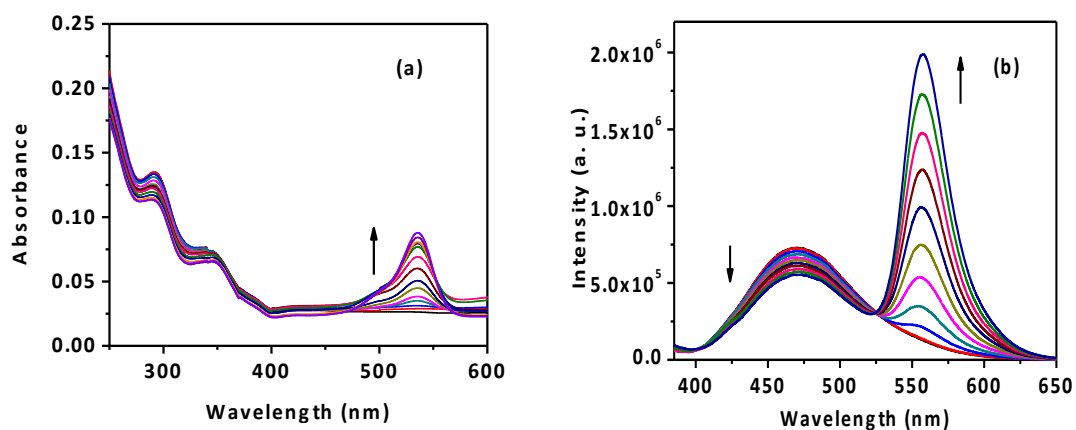


Figure S6: (a) The UV-vis spectra and (b) fluorescence spectra of RQBTE (10 μM, MeOH/H₂O, 1/4, pH=7.2) in presence of Fe³⁺ (0-2.5 equivalents in water).

4. ¹H NMR spectrum of compound 1

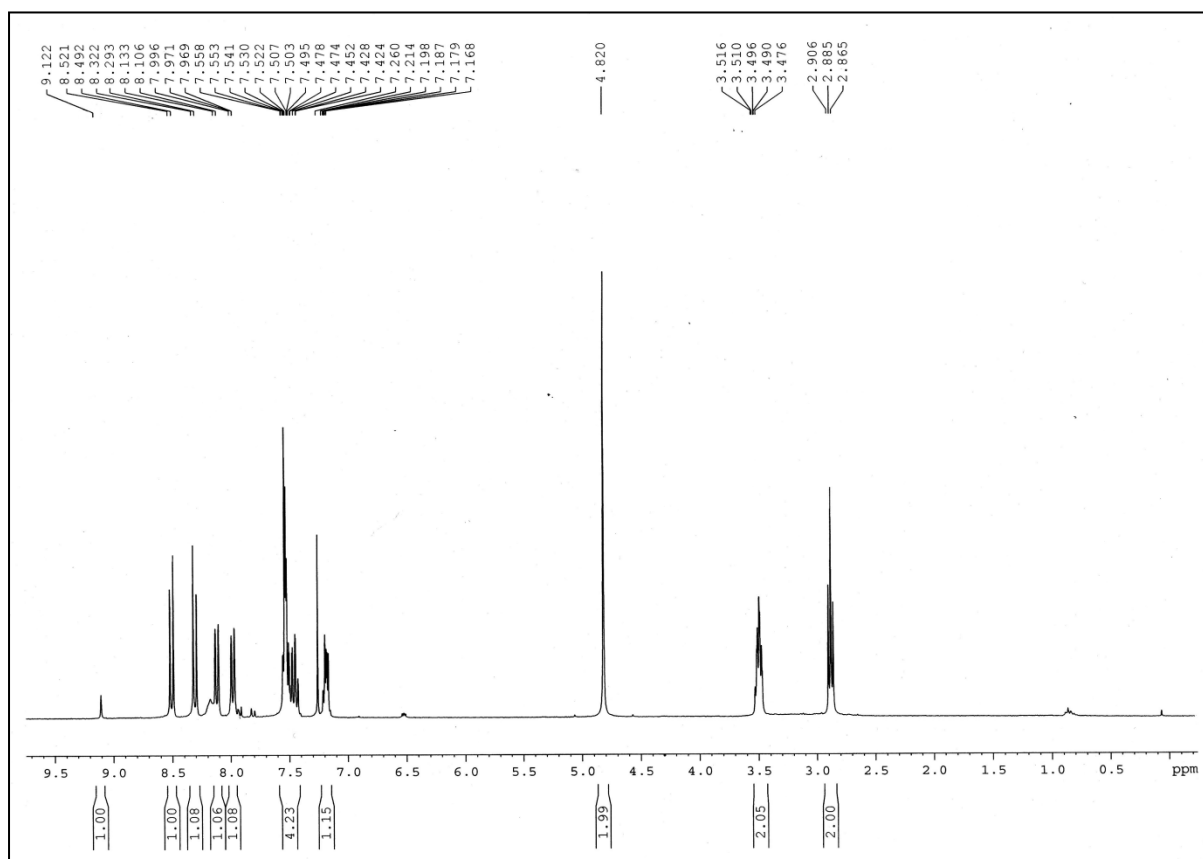


Figure S7: ¹H NMR (300 MHz) spectra of compound 1 in CDCl₃.

5. ^{13}C NMR spectrum of compound 1

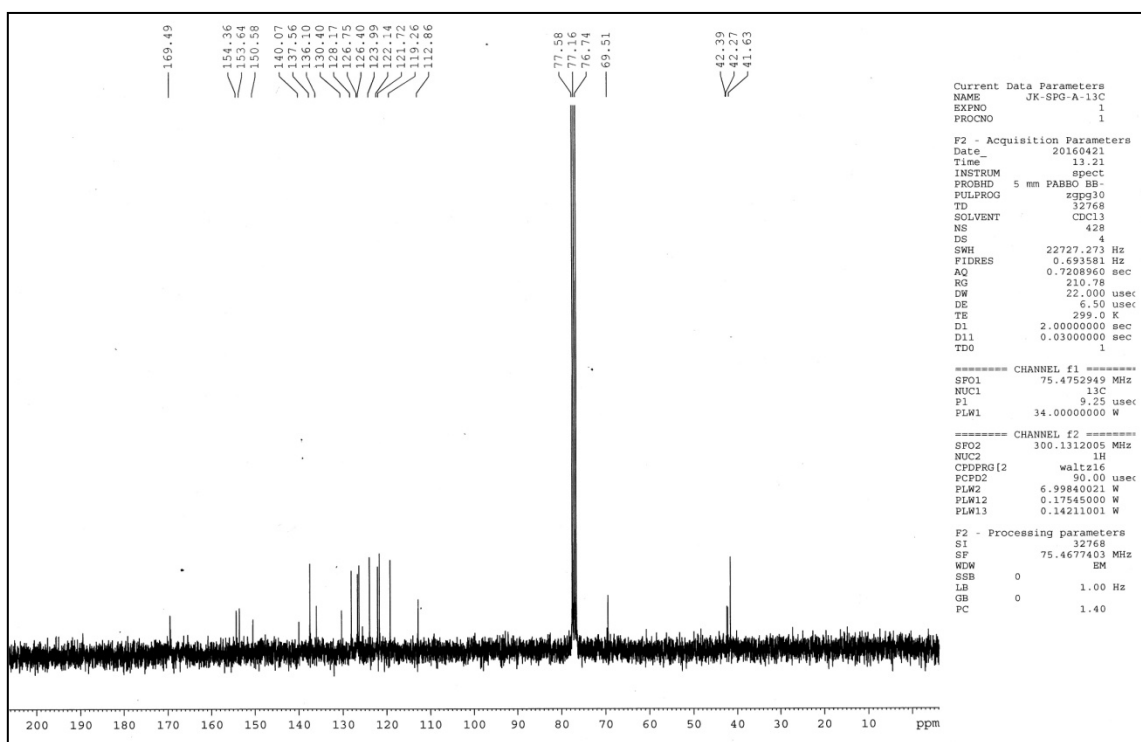


Figure S8: ^{13}C NMR (75 MHz) spectra of compound 1 in CDCl_3 .

6. Mass spectrum (HRMS) of Compound 1

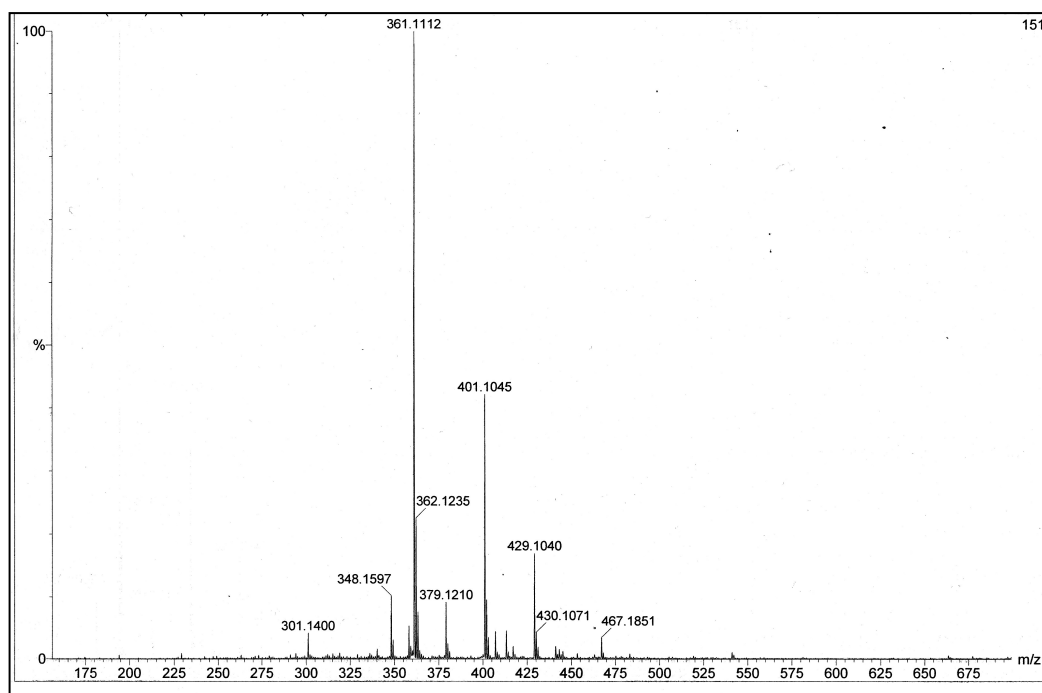


Figure S9: HRMS of compound 1.

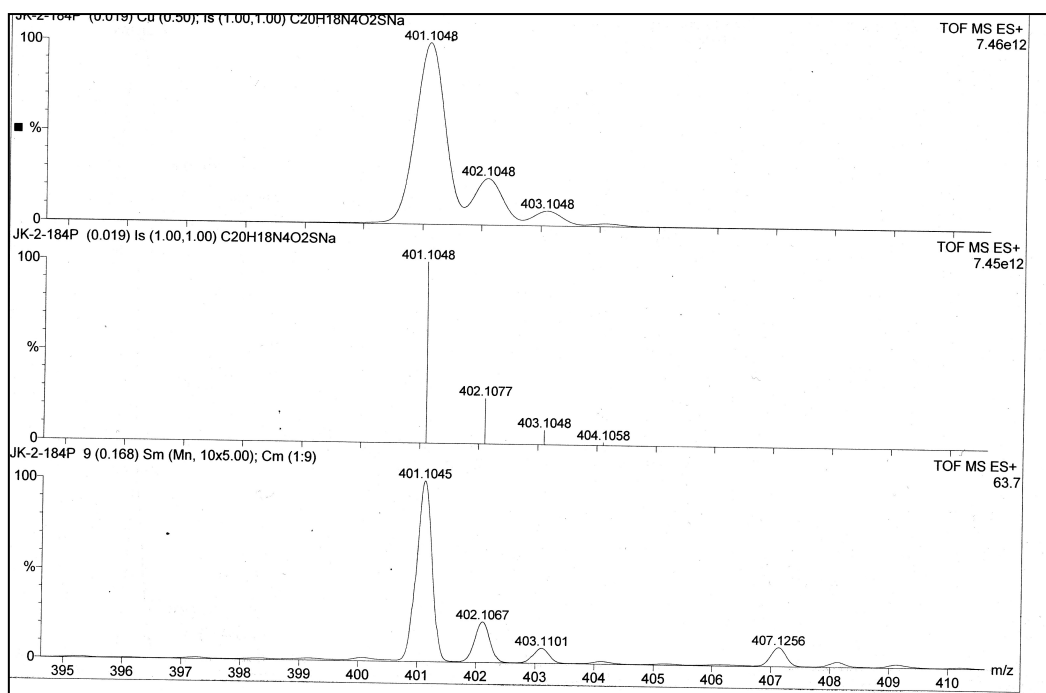


Figure S10: HRMS (expansion) of compound 1.

7. ^1H NMR (300 MHz) of RQBTE:

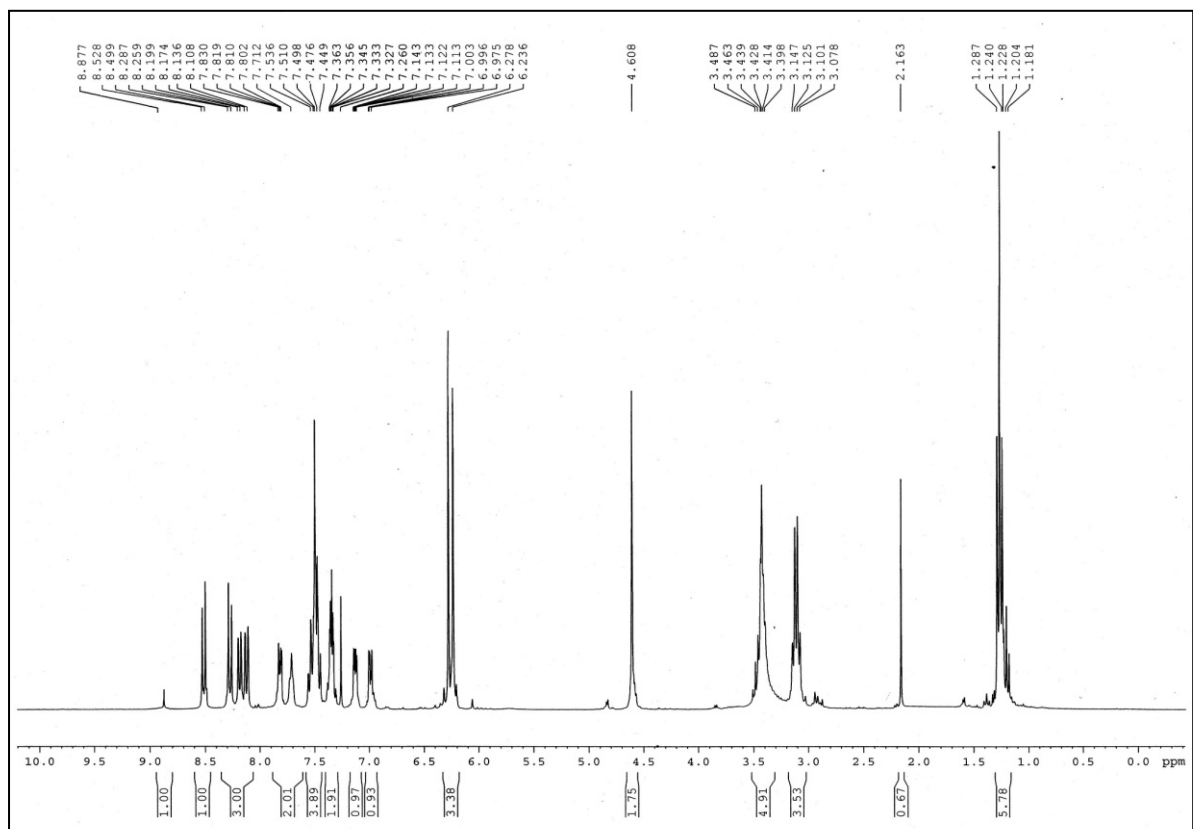


Figure S11: ^1H NMR (300 MHz) spectrum of RQBTE in CDCl_3 .

8. ^{13}C NMR spectrum of RQBTE

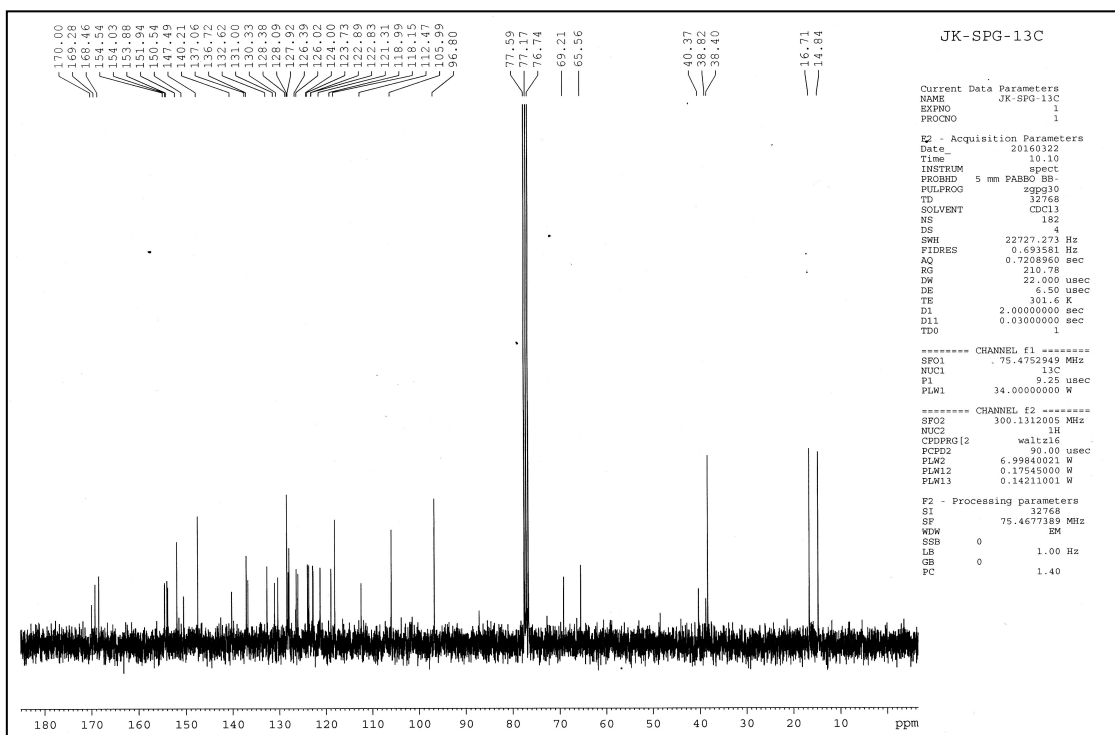


Figure S12: ^{13}C NMR (75 MHz) spectra of the receptor (RQBTE) in CDCl_3 .

9. Mass spectrum (HRMS) of RQBTE

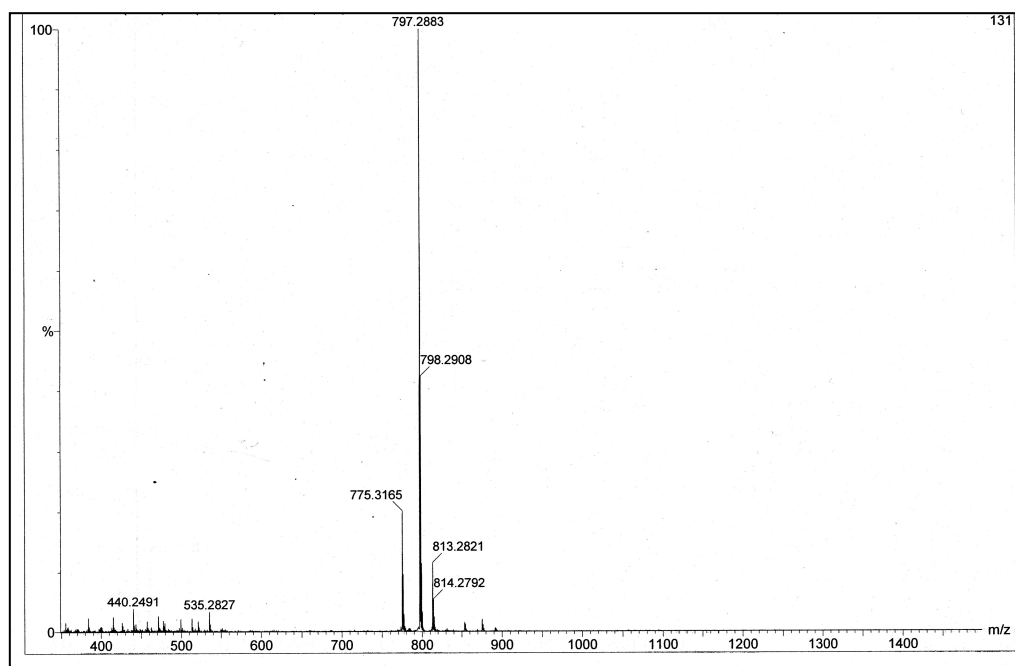


Figure S13: HRMS of RQBTE

10. HRMS of RQBTE-Fe³⁺ complex.

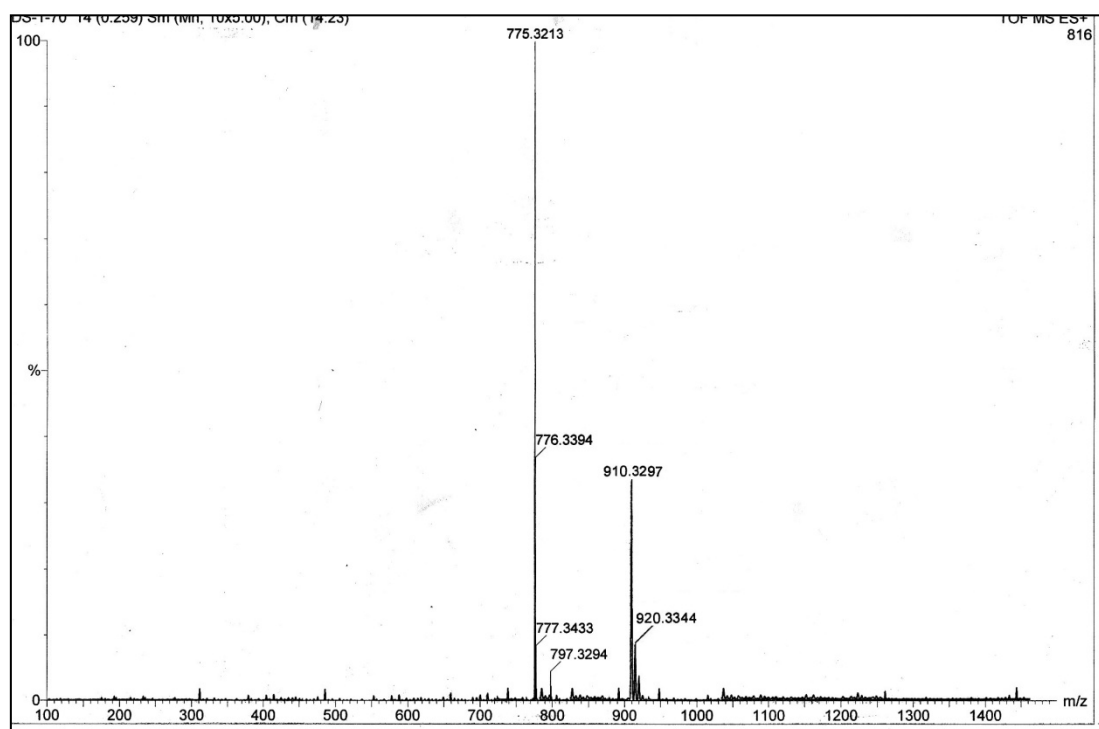


Figure S14: HRMS spectra of RQBTE-Fe³⁺ complex.

Table S3: The comparison of the present probe with recently reported probes for Fe³⁺ have been outlined in this table.

Fluorophore used	Type of response	Nature of enhancement	Detection limit	Reference
Anthracene	Colorimetric, fluorometric	Turn-on	5.8×10^{-7} M	<i>Chem. Commun.</i> , 2014, 50, 4631
Rhodamine-6G and 6-(hydroxymethyl)picolinohydrazide	Colorimetric, fluorometric	Turn-on	3.6×10^{-8} M	<i>Dalton Trans.</i> , 2013, 42, 15113
8-piperazino naphthalimide-rhodamine B	Colorimetric, Fluorometric	Ratiometric	5×10^{-8} M	<i>Analyst</i> , 2013, 138,1334.
Fluoranthene	Colorimetric, fluorometric	Turn-on	2.49×10^{-7} M	<i>Dyes and Pigments</i> , 2012, 94, 60
Rhodamine B, 8-Aminoquinoline and 2-aminopyridine	Colorimetric, fluorometric	Turn -on	3.5×10^{-6} M	<i>Dalton Trans.</i> , 2014, 43, 5983
Anthracene-benzimidazole	fluorometric	Ratiometric	Not given	<i>Tetrahedron Letters</i> , 2011, 52, 1368.
Aminoxy-linked rhodamine hydroxamate	Colorimetric, fluorometric	Turn-on	Not given	<i>Tetrahedron Letters</i> , 2010, 51, 3290.
4-(diethylamino) benzaldehyde-pyridine	Colorimetric, fluorometric	Ratiometric	5.8×10^{-8} M	<i>Dalton Trans.</i> , 2013, 42, 13889
4-(4-hydroxy-1-naphthylazo)benzenesulfonic acid	Colorimetric	-	4.2×10^{-9} mol L ⁻¹	<i>RSC Adv.</i> , 2014,4, 19370-19374
8-quinolinol- Rhodamine 6G hydrazide	Colorimetric, fluorometric	Ratiometric	Not given	<i>Org. Biomol. Chem.</i> , 2012, 10, 9634.
Thiacalix[4]arene	Colorimetric, fluorometric	Turn-off	5×10^{-7} M	<i>Dalton Trans.</i> , 2012, 41, 408.
Benzothiazole -quinoline - rhodamine-6G	Colorimetric, fluorometric	Ratiometric	5.39×10^{-8} M	Present Work

References

1. Cosier, J.; Glazer, A. M. A nitrogen-gas-stream cryostat for general X-ray diffraction studies. *J. Appl. Cryst.* 1986, 19, 105–107.
2. Bruker. APEX2, SAINT and SADABS. Bruker AXS Inc.: Madison, WI, USA, 2009.
3. Sheldrick, G.M. A short history of SHELX. *Acta Cryst.* 2008, A64, 112-122.